



A new approach to growth of chemically depositable different ZnS nanostructures

A. Goktas¹ · A. Tumbul^{1,2} · F. Aslan¹

Received: 22 January 2019 / Accepted: 1 April 2019 / Published online: 10 April 2019
© Springer Science+Business Media, LLC, part of Springer Nature 2019

Abstract

Different ZnS nanostructures synthesized by a chemical solution process were deposited on the glass substrate by dip coating technique. The effect of the sol-pH variation on the surface morphology, crystalline quality, optical band gap, and photoluminescence of the ZnS nanosphere, nanorod and mixed hexagonal cubic and rectangular-like nano-grains were investigated. It was found that the triethanolamine/ethanolamine played a key role to get desired nanostructure quality with different surface morphology. All nanostructures, derived in acidic and basic medium showed mixed cubic and hexagonal crystalline structure with preferred orientation along (111) plane of predominant cubic phase without oxidation. Nanospherical grains, sharply increased in size observed in acidic medium, whereas nanorods and mixed hexagonal, cubic and rectangular-like grains, slightly increased and then decreased in size, observed in basic medium with increased pH. The increased/decreased in average crystallite size was confirmed by reduced/enhanced dislocation density and micro strain. Comparatively, the band gap (E_g) of the nano-grains, reduced by pH derived in acidic medium was higher than those derived in basic medium. Comparatively, the higher surface defects related emission was observed in nanostructures derived in acidic medium than those derived in basic medium, whereas a higher green emission was observed in nanostructures fabricated at basic medium compared with the nanostructures synthesized in acidic medium. The results showed better crystalline quality in nano-grains derived at acidic medium than those derived at basic medium, whereas better optical quality in nanostructures derived at basic medium compared with the nanostructures derived at acidic medium. The observed characteristics are highly attractive for solar cells and optoelectronic applications.

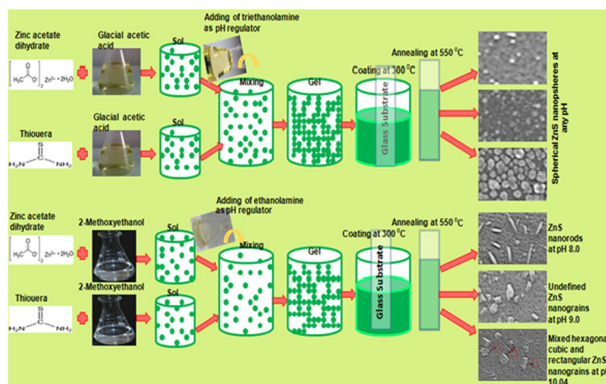
✉ A. Goktas
agoktas@harran.edu.tr

¹ Faculty of Science and Arts, Department of Physics, Harran University, Sanliurfa 63290, Turkey

² Central Laboratory, Harran University, Sanliurfa 63290, Turkey

Graphical Abstract

To get ZnS solution by chemical route, using glacial acetic (solvent) acid with triethanolamine (pH regulator) leads to the spherical ZnS nano-grains at any pH value, whereas using 2-methoxyethanol (solvent) with ethanolamine (pH regulator) brings about nanorods, undefined and mixed hexagonal, cubic and rectangular ZnS nano-grains at pH 8.0, 9.0, and 10.04, respectively.



Highlights

- Growth of chemically deposited different ZnS nanostructures.
- Formation of ZnS nanorods without using any capping agent at pH 8.0.
- A higher crystalline quality in ZnS nanostructures derived in acidic medium than the others.
- Comparatively a better optical quality in the ZnS nanostructures derived in basic medium than the others.
- Enhancement of the optical constants of the ZnS nanostructures as growing medium shifted from acidic to basic.

Keywords ZnS nano-grains · pH · Raman · Photoluminescence

1 Introduction

Recently, nano-grained semiconducting materials have gained a huge interest of the researchers for their extraordinary characteristics such as structural, optical, electrical, and electronics in various applications: LED's; flat-panel displays; sensors and lasers; non-linear optics; quantum, electroluminescence, and photovoltaic devices; and infrared windows [1–6]. In case of the nano-grained materials, some new physical effects can be observed with nano-grained thin films but bulk materials. Sometimes the physical properties can be depended on the functions of the nano-grain size in nano-grained structures. For example, when the nano-grain size of the nanostructures is comparable with the de Broglie wavelength of the electron, the quantization of the electron levels leads to new size effects.

Among the different II–IV semiconductors, ZnS has a broad spectrum of applications as denoted above and it has also wide band gap (3.60 eV) with an exciton binding energy of 40 meV. What's more, it is a non-toxic material and has n-type conductivity. Hence, it can be considered as a good buffer layer alternative to CdS and convenient for thin film solar cell based CdTe, CuInS₂, and CuGaIn(S,Se) [7, 8]. Furthermore, it has a high refractive index ($n \sim 2.3$), which can be used in antireflective coatings. Moreover, apart from these unique properties and marvelous versatility

in optoelectronic applications it is relatively the most stable compound with low toxicity. Nevertheless, at nanoscale, surface states can play an important role in luminescent characteristics and efficiency [9].

Till date, numerous technique have been used to synthesis ZnS nano-grains and to control their morphology and crystalline quality such as chemical solution (sol-gel) [10], chemical bath deposition (CBD) [11], spray pyrolysis [12], molecular beam epitaxy [13], sputtering [14], electro deposition [15], micro-emulsion [16], and capped precipitation [17] etc. The method of chemical solution is intensively used to obtain ZnS nanostructures due to its maneuverability, simplicity, low cost, reproducibility, facile procedure, and non-toxicity via used soft chemicals. Therefore, this is relatively one of the most preferred chemical methods to produce ZnS nanostructures due to the some difficulties within the CBD. It is highly attractive for the industrial production process, suggesting a relatively higher growing ratio through using low cost equipments, very quick and proper to fabricate nanostructures with a highly pure yield of starting raw materials.

To tune the morphology of the ZnS nano-grains different factors have been proposed. For example, chemical reactants [18], dopants [19], pH [20], growth rate [21], and deposition technique [22]. Among them the effect of the pH has been rarely investigated for the chemical solution derived ZnS thin films. Recently, Shayesta et al. [23] have

synthesized ZnS nanoparticles embedded in polyvinyl alcohol (PVA) matrix as capping agent for different pH (6–8) by using wet chemical process. The structural and optical characteristics were improved but no change in the surface morphology. More recently, Choudapur et al. [24] have reported the influence of the pH values (3–10) on the morphology, crystallinity, and optoelectronic properties of ZnS thin films and nanoparticles. However, no significant change in the surface morphology of the ZnS nanostructures but crystallinity and optical quality. After that, Akthar et al. [25] have also observed the change in optical properties of sol-gel derived ZnS thin films depended on pH values (1–7). Nonetheless, to the best of our knowledge research on the effect of the pH, which can significantly change the surface morphology (including nanorod, spherical, and rectangular-like nano-grains) of the ZnS nanostructures, has not been reported yet. A lot of the reported studies have used capping agent or modified chemical solution technique to get ZnS nanorods, spheres, etc. Most of them far from the physical meaning behind the formation of different surface morphologies including nanospheres, nanorods, and rectangular-like nano-grains. Therefore, in the current study we have studied the influence of the wide range pH variation (4–11) on the surface morphology, grain/crystallite size, optical properties including optical, and dielectric constants, as well as photoluminescence (PL) of the ZnS nano-grains in more detail, which is highly promised for the optoelectronic and solar cell applications.

2 Experimental

All precursors including zinc acetate dihydrate ($\text{Zn}(\text{CH}_3\text{CO}_2)_2 \cdot 2\text{H}_2\text{O}$), thiourea ($\text{CH}_4\text{N}_2\text{S}$), 2-Methoxyethanol ($\text{CH}_3\text{OCH}_2\text{CH}_2\text{OH}$), glacial acetic acid ($\text{CH}_3\text{CO}_2\text{H}$), and triethanolamine/ethanolamine ($\text{C}_6\text{H}_{15}\text{NO}_3/\text{C}_2\text{H}_7\text{NO}$) were of analytical grade, purchased from Merck company and used as received. 2-Methoxyethanol/glacial acetic acid and ethanolamine/triethanolamine were solvent and stabilizer, respectively, for preparation of the two type solution. Zinc acetate dihydrate and thiourea were used as starting salt powders to supply Zn^{2+} and S^{2-} ions. In all, 0.2 M $\text{Zn}(\text{CH}_3\text{CO}_2)_2 \cdot 2\text{H}_2\text{O}$ and 0.8 M $\text{CH}_4\text{N}_2\text{S}$ were dissolved in 20 ml of 2-Methoxyethanol (solution I); 0.2 M $\text{Zn}(\text{CH}_3\text{CO}_2)_2 \cdot 2\text{H}_2\text{O}$ and 0.8 M $\text{CH}_4\text{N}_2\text{S}$ were dissolved in glacial acetic acid (solution II). These two mixtures were stirred for 20 min on magnetic stirrer at room temperature to get clear and highly transparent solutions. To regulate the pH of the each mixture, the different amount of the ethanolamine (for solution I) and triethanolamine (for solution II) were used for basic (pH = 8, 9, 10, and 11) and acidic (pH = 4, 5, and 6) conditions, respectively. After regulating the pH of the total mixtures, they were continuously stirred for 24 h to get

the final solutions. To obtain desired nano-grains/nanostructures, the final solutions were dip coated on the properly cleaned glass sample holders by dip coating system at 300°C in air conditions. By this process, the sample holders were deposited 10 times to get the intended thickness. The deposited ZnS nano-grains were subjected to the post-heat treatment at 550°C in argon environment (Fig. 1).

In order to identify the crystal structure of the ZnS nano-grains, the X-ray powder diffraction (XRD) type of Rigaku Ultima III (40 kV, 30 mA, and 1.54 \AA) power diffractometer was employed. Surface morphologies were carried out by scanning electron microscopy (SEM, Zeiss Evo 50). To investigate the vibration characteristics of the produced nanostructures Raman spectrophotometer was used (excitation wavelength = 785 nm). PL study was employed by using Hitachi F-2500 FL spectrophotometer. Optical characterizations including absorption and transmission spectrums were performed by Ultraviolet-visible (UV-vis) spectroscopy (Perkin Elmer 45) in the wavelength range of 300–900 nm.

Dislocation density (δ) and micro strain (ϵ) of the ZnS nano-grains are calculated by following relations:

$$\delta = \frac{1}{D_{hkl}} \quad (1)$$

$$\epsilon = \frac{\beta}{4\tan\theta} \quad (2)$$

where β shows the full width at half of the peak maximum (FWHM), λ is the wavelength of incident X-ray, and θ represents Bragg's angle.

Band gap energy (E_g) of the nanostructures can be obtained by using the following equation:

$$\alpha h\nu = A(h\nu - E_g)^n \quad (3)$$

where α is known as absorption coefficient, n can variable as 1 or $1/2$ in case of the direct or indirect transitions, respectively, h represents the Planck's constant and ν is the photon frequency.

3 Results and discussion

3.1 Surface morphology and composition analysis

The surface morphology of the nanostructures is shown in Fig. 2a–d and Fig. 3a–f for the acidic and basic conditions with different pH values, respectively. As seen in Fig. 2a–d, a spherical nano-grain is observed for acidic conditions, in which grain size of the particles (approximately ranging between 20 and 60 nm) increases as the pH value increases from 4 to 6.1. The attractive forces within ZnS nanostructures bring about the aligning of the particles with perfect coordination, which resulted in eliminated common

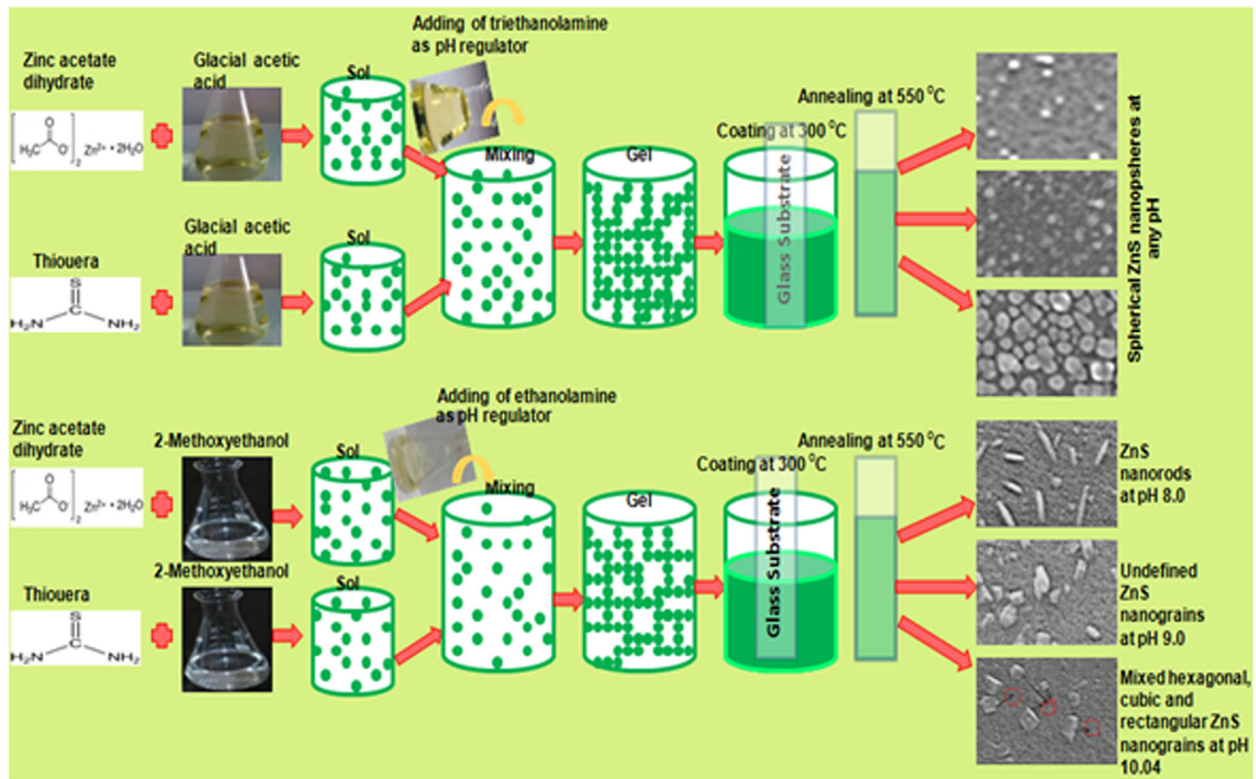


Fig. 1 Schematic presentative of chemically deposit details for different type of ZnS nano-grains

Fig. 2 Scanning electron microscopy (SEM) images of ZnS nano-grains at acidic medium with pH of 4 **a**, 5.3 **b**, 6.2 **c**, and cross-section at pH 6.1 **d**

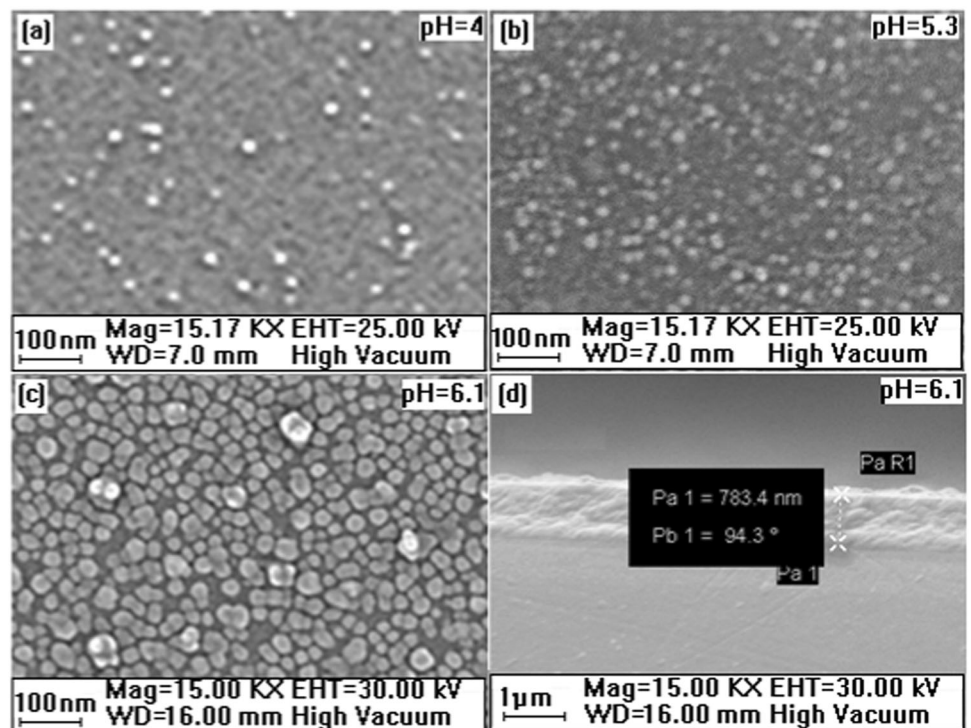
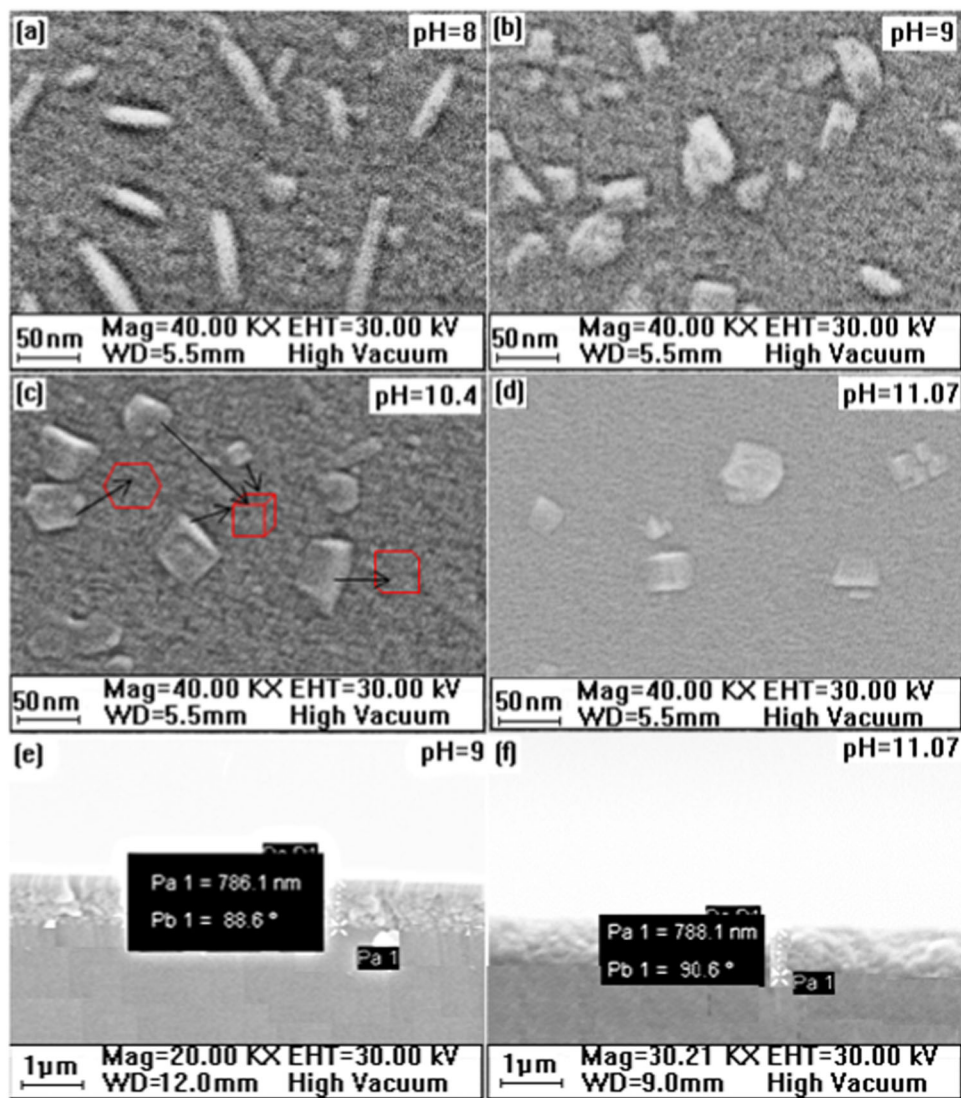


Fig. 3 Scanning electron microscopy (SEM) images of ZnS nano-grains at basic medium with pH of 8 **a**, 9 **b**, 10.4 **c**, 11.07 **d**, and cross-sections at pH 9 **e** and 11.07 **f**

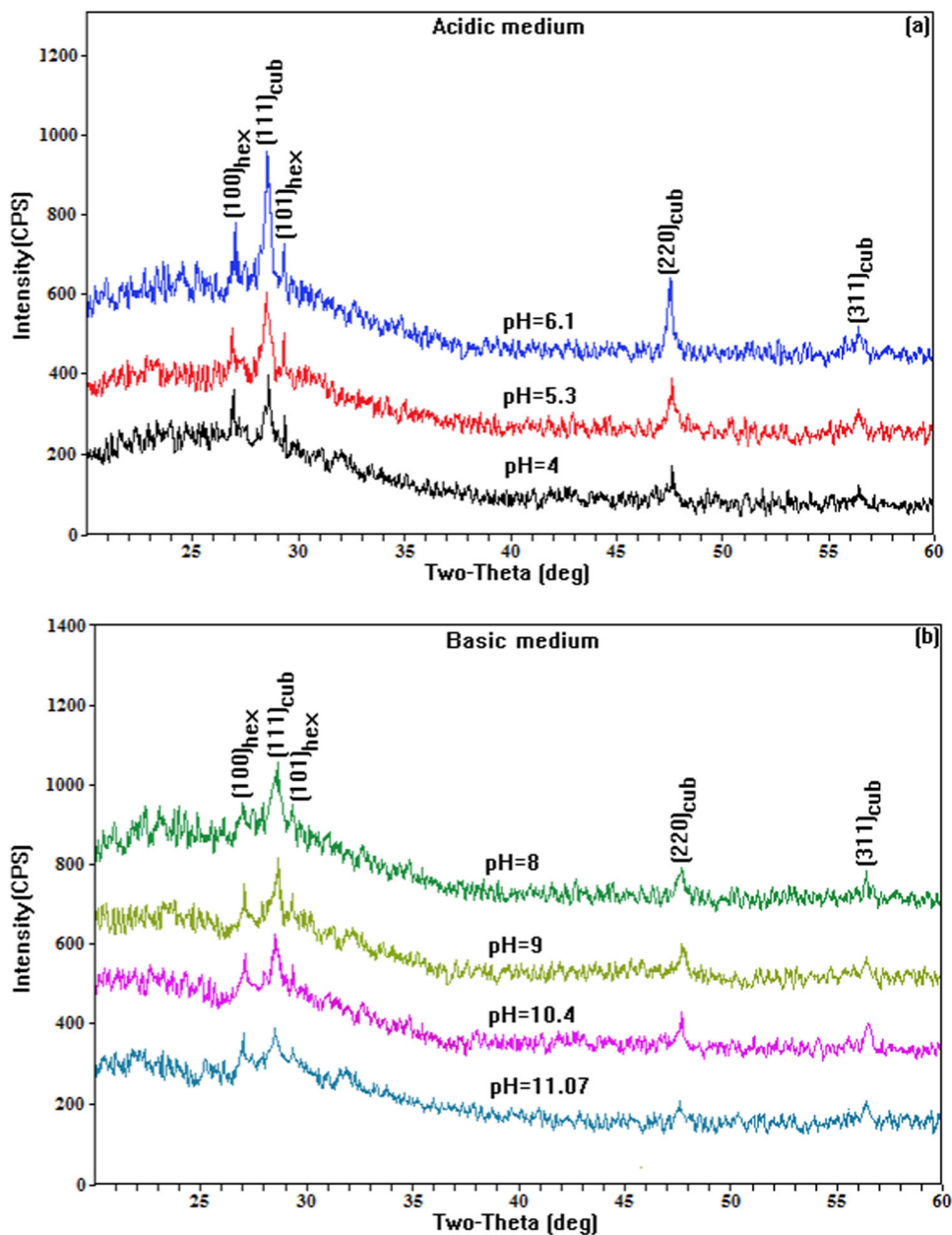


boundaries and then the formation of big particles with well-defined morphology [26]. This idea is also supported by XRD measurements as given in Fig. 4a. Compared with the basic conditions, there is no significant change in the surface morphology of the nanostructures synthesized in acidic conditions with increased pH value. However, it is noteworthy to note that there is a remarkable change in surface morphology of ZnS nano-grains derived in basic conditions with increased pH values from 8 to 11.07 (Fig. 3a–f). The surface morphology of well-defined nanorods, having sizes is between about 25–150 nm was observed at pH 8.0 (Fig. 3a). At pH 9.0, it is found that the heterogeneous film surface with undefined grains with sizes varying about 10 to 50 nm (Fig. 3b). Enhancing pH at 10.4, it can be seen that well-defined clusters having mixed hexagonal, cubic, and rectangular grains with sizes between about 10 and 50 nm (Fig. 3b). At pH 11.07, approximately

the same clusters as those obtained at pH of 10.4, nevertheless these are smaller in size, non-compact and have less dense surface grains compared with the pH 10.4. This is also proved by XRD measurements in which higher average crystalline quality is obtained for the nanostructures with pH 10.4 than that of with pH 11.07.

For the pH range 9.0–11.07, the surface morphology consists of the particles having rectangular, hexagonal, and cubic crystallite shapes. Compared with the pH 8.0, this new grain shapes is probably related to the increment of (100) crystal plane direction with respect to the (111) plane direction. The similar observations have been also reported for chemically derived CuO_2 nanostructures [26]. Comparatively, the higher surface grain sizes are observed for the acidic conditions than that of the basic conditions. Moreover, the surface morphologies of the nanostructures derived at acidic medium are uniform and there was no

Fig. 4 X-ray powder diffraction (XRD) pattern of ZnS nano-grains at acidic medium **a**, basic medium **b** at different pH values



change in the shape of spherical nano-grains but in size. However, in case of nanostructures derived at basic medium nanorods (at pH 8.0) and mixed rectangular, cubic, and hexagonal-like particles are found (at pH range 9.0–11.07). Compared with the ZnS nanostructures derived at acidic medium, there is no improvement in grain size of the ZnS nanostructures synthesized in basic medium as pH increased, which is likely connected to the reduced atomic density and increased porosity of the layers after critical pH 8.0 [27].

The origin of these different surface morphologies in ZnS nano-grains is attributed to the large difference between the surface energy of the non-polar (110) and the polar (111)

planes [28]. It is reported that the used chemical precursors [18] can also result in different surface morphologies due to the variation in surface energy. In addition, the formation of the $\text{Zn}(\text{OH})_4^{2-}$ anion, which is the main factor for the formation of the nanorods and depends on pH value [29]. Moreover, Hafeez et al. [30] have reported that the formation of the ZnS nanobelts and spherical nano-grains are depended on the effective chemical tension, which is served for Gibbs free energy. Accordingly, the formation of the different surface morphologies in ZnS nano-grains is probably related to the different surface energy of the different crystalline orientation plane, which strictly depends on the above-mentioned factors.

3.2 XRD analyses

The XRD patterns of the ZnS nano-grains derived at acidic and basic mediums with different pH values are presented in Fig. 4a, b, respectively. It is seen that all nano-grains have the pure ZnS phase with mixture hexagonal wurtzite (JCPDS Card No. 36-1450) and cubic sphalerite structure (JCPDS Card No. 05-0566), which are highly oriented along (111)_{cub} plane. The presence of the other diffraction peaks corresponding to (100)_{hex}, (101)_{hex}, (220)_{cub}, and (311)_{cub} planes, indicating the polycrystalline nature of the films and predominance of the cubic sphalerite structure. This fact was also previously observed [18, 31]. It is found that among observed all planes, the (111)_{cub} plane has the most intensive peak at pH 6.1 in the nanostructures derived at acidic medium reflecting well-improved crystalline quality of the ZnS nano-grains. To confirm this, the average crystallite (D_{hkl}) size of the samples was calculated by using Debye Scherrer's formula and the obtained values are given in Table 1. The D_{111} of the ZnS nanostructures derived from acidic medium is comparatively higher than those derived from basic medium. It is found that the grain size of the produced ZnS nano-grains is higher than the D_{111} due to the fact that grains are composed of many crystallites. As seen in Table 1, there is a very small decrease in the lattice parameters (for cubic system $a = b = c$) of the nano-grains derived in acidic medium. However, the lattice constants of the nanostructures derived at acidic medium are slightly enhanced by pH connected to the accommodation of the atoms within the crystal leads to relaxation of the crystal lattice. These values are in well agreement with the standard value (0.540 nm) reported in JCPDS Card No. 05-0566. It is found that the δ and ϵ are decreased by increasing pH of the acidic medium, reflecting improved crystalline quality of the nanostructures (Table 1). However, they have high values for the nanostructures derived in basic medium compared with acidic medium. This reflects worsening the crystalline quality of the ZnS nanostructures by changing pH from 8.0 to 11.07 at basic medium.

3.3 Raman analyses

Raman spectroscopy performed at room temperature was used to obtain information about molecular vibrations and other structural features such as the crystallinity of ZnS nanoparticles and their secondary phases. The observed Raman scattering spectra of the ZnS nano-grains were illustrated in Fig. 6a, b. The mean peaks centered at 217, 349, and 658 cm^{-1} are founded for the ZnS nanostructures (Fig. 5a, b). The observed Raman peak at 217 cm^{-1} is likely attributed to the tiny formation of $\text{C}_6\text{H}_{24}\text{N}_6\text{O}_4\text{SZn}$ with in ZnS nanostructures [18]. Another Raman peak at 349 cm^{-1} is identified as A1 and E1 symmetry longitudinal optic (LO)

Table 1 Summary of some structural values of FWHM, 2-theta, average crystallite size, lattice parameter, dislocation density, and micro strain for ZnS nano-grains at different pH values

pH value	FWHM (β_{002}°)	2 θ (deg.)	D(nm) ₁₁₁	a (nm)	δ ($\times 10^{-3}$)	ϵ ($\times 10^{-3}$)
4	0.98	28.56	8.9	0.5413	112	962
5.3	0.82	28.54	10.6	0.5420	94.3	806
6.1	0.58	28.54	15	0.5423	66	570
8	1.74	28.60	5	0.5408	200	1711
9	1.08	28.62	8	0.5406	125	1062
10.04	1.24	28.64	7	0.5404	142	1214
11.07	1.45	28.66	6	0.5402	166	1420

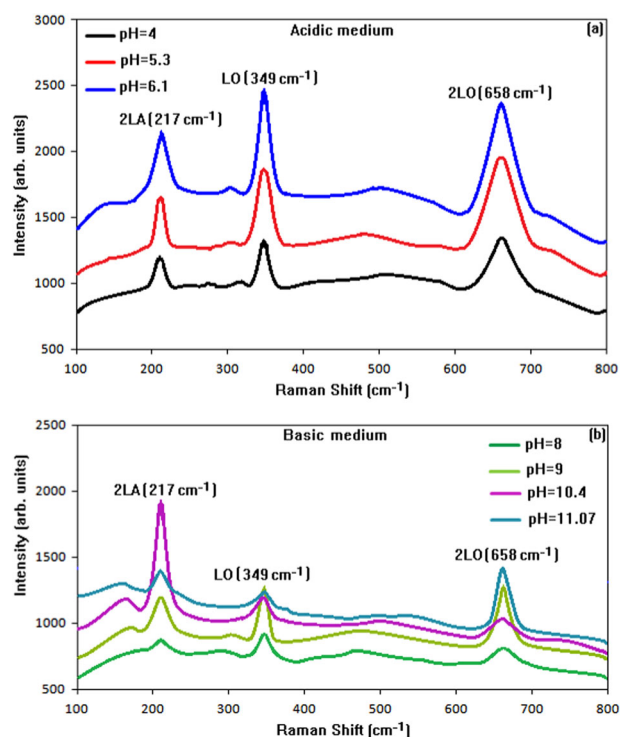


Fig. 5 Raman spectrum of ZnS nano-grains at acidic medium **a**, basic medium **b** at different pH values

mode. A relatively broad Raman peak at 658 cm^{-1} is assigned for the second ordered 2LO mode [32] assigned for combination and overtone scattering at high two-phonon density of state. The Raman peak intensities are increased with increasing pH at acidic medium indicating improved crystalline quality of the ZnS nano-grains as supported by XRD and SEM analyses. However, at basic medium, the observed main Raman peak intensities are comparatively lower than that of acidic medium suggest worsening the crystalline quality of the ZnS nano-grains derived from basic medium (Fig. 5b). Apart from these observations, the intensities of the main Raman peaks observed for the ZnS

nanostructures at basic medium probably due to the variation in surface morphologies. For example, at pH 8.0 the most intensive peak is observed for the 349 cm^{-1} peak position identified as A1 and E1 symmetry LO mode. However, at pH 10.4 the Raman peak observed for 2LA optical mode phonons has the most intensive peak among the others. Furthermore, at pH 9.0 and 11.07, the highest peak intensity is observed for the 2LO mode. These results suggest that the different peak intensities for the observed optical modes is likely due to the variation in surface morphology as proved by SEM analysis, where the preferred crystallite orientation degree is different for the different pH values especially in the ZnS nano-grains produced at basic conditions and they have different grain shapes, respectively. The observed results are in well agreement with the study on different surface morphology of the ZnS nanostructures synthesized by solvothermal technique using different reactants [18].

3.4 Optical characterizations

3.4.1 Uv-vis measurements

The room temperature Uv-vis transmittance spectra of the ZnS nano-grains with different pH values for the acidic and basic mediums are given in Fig. 6a, b. The nanostructures grown at basic medium show sharper fundamental

absorption band edge and higher average transmittance in the Uv-vis range approximately over than 80% than those of grown in acidic medium reflecting the better homogeneity and uniformity of the nano-grains than those grown in acidic medium. These results are comparable with high quality spray prolysis ZnS nanostructures [33] and notably better than previously reported results on ZnS nanostructures by many researchers [22, 24, 33–35]. So, such nano-grains can be used as attractive candidate materials for using as a buffer layer for the chalcopyrite photovoltaic solar cells, as well as several applications of the optoelectronic devices. Comparatively, the more pronounced oscillation in the transmission of the ZnS nano-grains derived from basic medium (see Fig. 6b) are observed indicating well homogeneity and thickness uniformity. The variation curves of $(\alpha h\nu)^2$ and $h\nu$ for the ZnS nano-grains are given in Fig. 7a, b, upon on different pH values at acidic and basic medium, respectively. The linear variation of the curves exhibits the presence of the direct transition. The band gap energy (E_g) of the nanostructures is found by extrapolation of the linear part of the curve between $(\alpha h\nu)^2$ and $h\nu$. As seen from Fig. 7a, b, the E_g of the nanostructures derived from acidic medium decreases with increasing pH value, whereas it increases for the nano-grains synthesized in basic medium (see Table 2). In both cases, the E_g values of the nano-grains are lower than that of bulk ZnS ($E_g \sim 4.08\text{ eV}$), indicating the quantum size effect in the ZnS nano-grains.

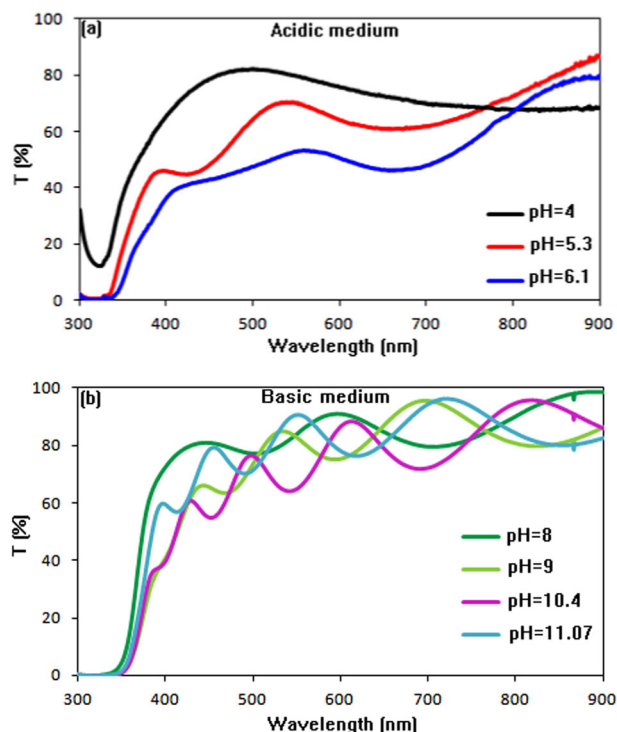


Fig. 6 Transmission spectra for ZnS nano-grains at acidic medium **a**, basic medium **b** at different pH values

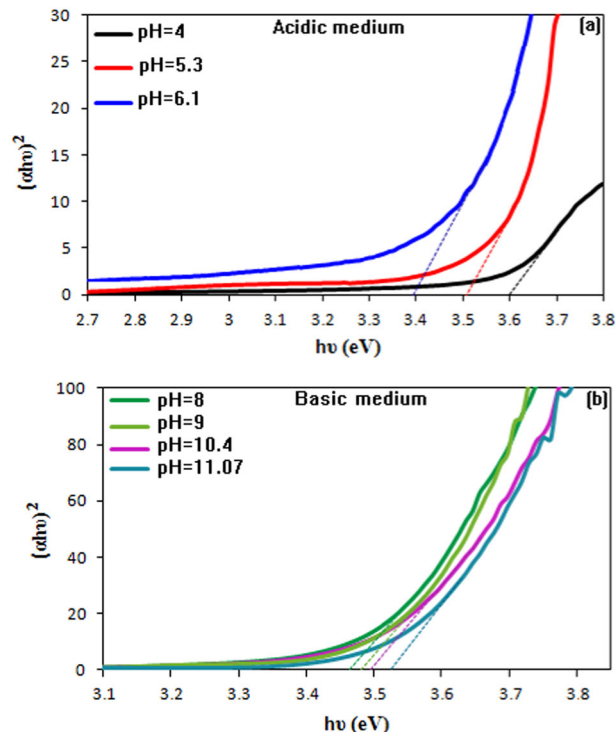


Fig. 7 The plots of $(\alpha h\nu)^2$ vs. $(h\nu)$ for ZnS nano-grains at acidic medium **a**, basic medium **b** at different pH values

Table 2 The variation of pH values versus optical band gap

pH value	E_g (eV)
4	3.600
5.3	3.506
6.1	3.394
8	3.446
9	3.483
10.04	3.494
11.07	3.525

The obtained E_g values are in well agreement with previous studies on ZnS nanostructures [22, 24, 31, 33]. It is well known that increasing/decreasing of the E_g is related to the decrease/increase in the lattice parameters and grain size of the materials. In case of the ZnS nanostructures derived from acidic medium, the increase in D_{111} and lattice parameter (a) results in reduced E_g values, whereas decreasing in them leads to the enhancement of the E_g values for the nano-grains produced at basic medium. This is due to the fact that a decrease/increase in a causes decreased/increased inter atomic distance, which brings about reduced/enhanced binding forces of the valance electrons. This reflects the less/more energy requires moving the electrons from the valance to the conduction band, then reducing/enhancing the E_g value.

The optical reflectance spectra of the ZnS nano-grains at room temperature are given in Fig. 8a, b. It is obvious that all the nano-grains have the reflectance <25%. The difference in the reflectivity of the nanostructures is likely due to the different transmittance and absorbance of the films caused by different surface morphology and grain size or D_{111} . As seen in Fig. 8a, the reflectance increases as pH value increasing from 4 to 6.1 in acidic medium, the same trend is also observed for the nanostructures derived from basic medium except for the pH at 11.07. Among all nanostructures, the highest reflectivity is observed for the nanostructure with pH 6.1 and 10.4 in acidic and basic medium, respectively. This is probably related to poor transparency in the visible range. Comparatively, the nano-grains derived at basic medium have higher reflectivity, at near ultraviolet region (between 300 and 400 nm) than those of derived at acidic medium.

3.4.2 PL measurements

To investigate the luminescence characterizations for the presence of defects related to green blue emissions bands, room temperature PL spectra, at wavelength range of 350–700 nm, for the nano-grains, which are produced at acidic and basic mediums are presented in Fig. 9a, b,

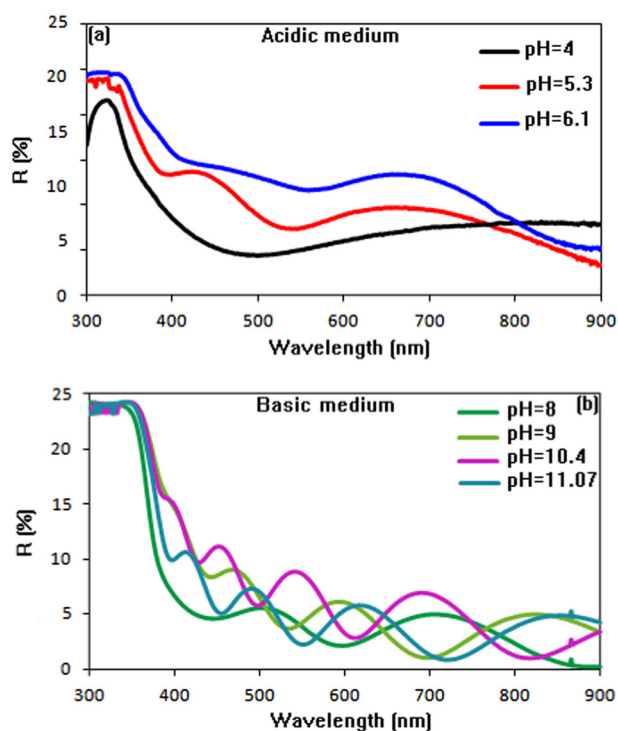


Fig. 8 Reflectance spectra for ZnS nano-grains at acidic medium **a**, basic medium **b** at different pH values

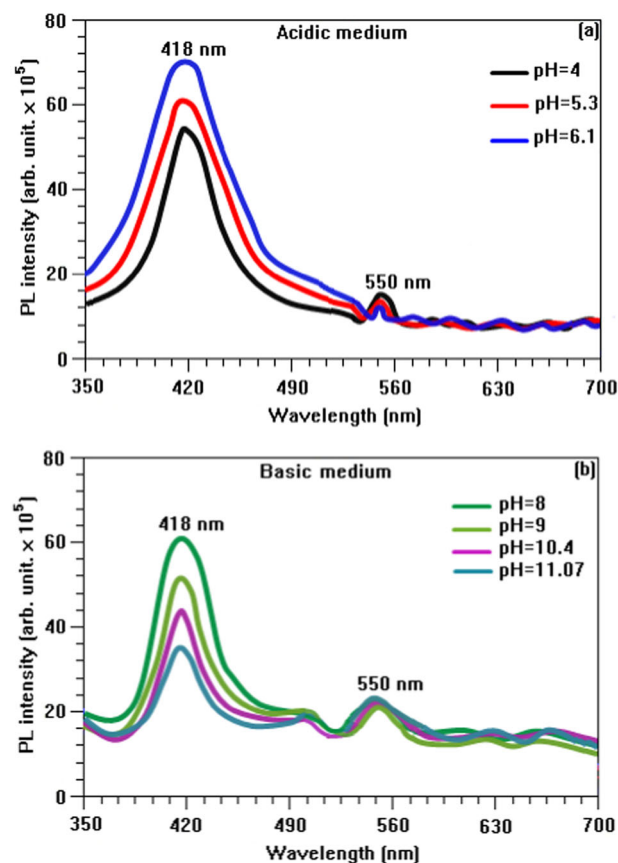


Fig. 9 Photoluminescence spectra of ZnS nano-grains at acidic medium **a**, basic medium **b** at different pH values

respectively. The spectra were obtained by using an excitation wavelength of 344 nm. It is obviously observed that there are two main peaks centered at 418 and 550 nm for the ZnS nanostructures derived from both mediums. The first one is attributed to the formation of the surface defect states of ZnS nanostructures [19]. Its energy is relatively lower than the E_g (3.39–3.60 eV) of produced ZnS nano-grains. The second one is probably due to the formation of Zn or S vacancies [36].

As can be seen in Fig. 9a, as the pH increases the relative intensity of the peak located at 418 nm also increases, however, the relative peak intensity of 550 nm emission has decreased confirming the improved the nanocrystalline quality of ZnS nanostructures, being best at pH 6.1 (Table 1). The opposite trend has also been observed for the nano-grains synthesized in basic conditions. The increased emission intensity at 550 nm reflects the worsening nanocrystalline quality of the nanostructures derived from basic medium as pH enhanced due to the formation of more crystalline defects (Table 1).

Comparatively, the higher PL is observed at 418 nm for the ZnS nano-grains derived from acidic medium, whereas at 550 nm the higher and broader PL emissions are observed for the nano-grains derived from basic medium (Fig. 9a. b). By changing pH at both medium, the peak position of 550 nm slightly shifts to higher/lower energies likely due to the variation in OH⁻ concentration or the variation in sulfur content has been reported [36].

4 Conclusions

A comparative study on the structural, optical and PL characterizations of ZnS nano-grains with nanospherical, nanorods, mixed hexagonal, cubic, and rectangular-like nanostructures were successfully fabricated on glass substrates by chemical solution route in acidic and basic mediums with wide range sol-pH variation was presented. It was found that the ethanalamine and triethanolamine played a critical role to obtain ZnS nanostructures with different surface morphology and crystalline quality, as well as optical quality.

ZnS nanostructures produced in both of the medium had mixed cubic and hexagonal crystalline structure having preferred orientation along (111) plane of predominant cubic phase. With increased pH, the average crystalline quality of nano-grains derived in acidic medium enhanced, which was supported by reduced dislocation density and micro strain compared with the nano-grains derived in basic medium. The lattice parameter was also increased for the nanostructures synthesized in the acidic medium while it slightly decreased for the nano-grains produced in basic medium.

The variation of the lattice parameter/average crystallite size was also supported by the band gap energy of the nanostructures, which was decreased/increased for the nanostructures derived at acidic medium while it increased/decreased for the nano-grains synthesized at basic medium as pH increased. A relatively higher and broad green emission was detected for the nano-grains derived at basic medium with respect to the nano-grains obtained at basic medium, whereas the higher surface defects related emission was observed for the nano-grains derived from acidic medium than those derived at basic medium. Compared with the nano-grains derived at acidic medium, the better optical quality was found for the nano-grains derived in basic medium, whereas they had impaired crystalline quality.

The observed results are in good agreement with previous reports on ZnS nanostructures produced by different techniques. In addition, this is the first systematic and comparative study on the structural, optical, and PL properties of the ZnS nano-grains, as well as the first observation of different surface morphology of ZnS nanostructures with nanosphere, nanorod, and mixed hexagonal cubic and rectangular-like nano-grains produced by chemical solution and dip coating process without using any capping agent and other reactants or equipments to get nanorods. The observed results on the ZnS nano-grains might have a potential application in chalcopyrite-based photovoltaic solar cells and optoelectronic field.

Acknowledgements Financial support from the Scientific Research Project Commission of Harran University (HUBAK) under Project No. 18062 is gratefully acknowledged.

Compliance with ethical standards

Conflict of interest The authors declare that they have no conflict of interest.

Publisher's note: Springer Nature remains neutral with regard to jurisdictional claims in published maps and institutional affiliations.

References

- Zhu Y-P, Li J, Ma T-Y, Liu Y-P, Du G, Yuan Z-Y (2014) Sonochemistry-assisted synthesis and optical properties of mesoporous ZnS nanomaterials. *J Mater Chem A* 2:1093–1101
- Datta S, Kabir M, Saha-Dasgupta T (2012) Effects of shape and composition on the properties of CdS nanocrystals. *Phys Rev B* 86:115307
- Fang X, Wu L, Hu L (2011) ZnS nanostructure arrays: a developing material star. *Adv Mater* 23:585–598
- Fang X, Zhai T, Gautam UK, Li L, Wu L, Bando Y, Golberg D (2011) Recent advances in zinc sulfide nanostructures. *Prog Mater Sci* 56:175–287

5. Ziegler J, Shu X, Kucur E, Meister F, Batentschuk M, Gindele F, Nann T (2008) Silica-coated InP/ZnS nanocrystals as converter material in white LEDs. *Adv Mater* 20:4068–4073
6. Liu X, Cai X, Mao J, Jin C, Liu X, Cai X, Mao J, Jin C (2001) ZnS/Ag/ZnS nano-multilayer films for transparent electrodes in flat display application. *Appl Surf Sci* 183:103–110
7. Velumani S, Ascencio JA (2003) Characterization of ZincPhthalocyanine (ZnPc) for photovoltaic applications. *Appl Phys A Mater Sci Process* 72:236–247
8. Luo P-F, Jiang G-S, Zhu C-F (2009) Pulsed laser deposition ZnS buffer layers for CIGS solar cells. *Chin J Chem Phys* 22:97–101
9. Sookhakian M, Amin YM, Basirun WJ, Tajabadi MT, Kamarulzaman N (2014) Synthesis, structural, and optical properties of type-II ZnO-ZnS core-shell nanostructure. *J Lumin* 145:244–252
10. Goktas A (2015) Sol-gel derived $Zn_{1-x}Fe_xS$ diluted magnetic semiconductor thin films: compositional dependent room or above room temperature ferromagnetism. *Appl Surf Sci* 340:151–159
11. Nakada T, Mizutani M, Hagiwara Y, Kunioka A (2001) Improvement of CIGS thin-film solar cell performance by optimization of Zn(O,S) buffer layer parameters. *Sol Energy Mater Sol Cells* 67:255–260
12. Hichou AEL, Addou M, Bubendorff JL, Ebothe J, Idrissi BEL, Troyon M (2004) Microstructure and cathodoluminescence study of sprayed Al and Sn doped ZnS thin films. *Semicon Sci Technol* 19:230–235
13. Liu Q, Guobing M, Jianping A (2008) Chemical bath-deposited ZnS thin films: preparation and characterization. *Appl Surf Sci* 254:5711–5714
14. Shao LX, Chang KH, Hwang HL (2003) Zinc sulfide thin films deposited by RF reactive sputtering for photovoltaic applications. *Appl Surf Sci* 212–213:305–310
15. Mane RS, Lokhande CD (2000) Chemical deposition method for metal chalcogenide thin films. *Mater Chem Phys* 65:1–31
16. Charinpanitkul T, Chanagul A, Dutta J, Rungsardthong U, Tanthapanichakoon W (2005) Effects of cosurfactant on ZnS nanoparticle synthesis in microemulsion. *Sci Technol Adv Mater* 6:266–271
17. Rahdar A (2013) Effect of 2-mercaptoethanol as capping agent on ZnS nanoparticles: structural and optical characterization. *J Nanostruct Chem* 3:10–15
18. Gao W, Cao M, Xiao W, Lei F, Huang J, Sun Y, Wang L, Shen Y (2016) Effects of reaction conditions on the structural, morphological and optical properties of solvothermal synthesized ZnS nanostructures. *Mater Sci Semicon Process* 56:349–356
19. Goktas A, Mutlu İH (2016) Structural, optical, and magnetic properties of solution-processed co-doped ZnS thin films. *J Elec Mater* 45:5709–5721
20. Luque PA, Castro-Beltran A, Vilchis-Nestor AR, Quevedo-Lopez MA, Olivas A (2015) Influence of pH on properties of ZnS thin films deposited on SiO₂ substrate by chemical bath deposition. *Mater Lett* 140:148–150
21. Antony A, Murali KV, Manoj R, Jayaraj MK (2005) The effect of the pH value on the growth and properties of chemical-bath-deposited ZnS thin films. *Mater Chem Phys* 90:106–110
22. Ben Nasr T, Kamoun N, Kanzari M M, Bennaceur R (2006) Effect of pH on the properties of ZnS thin films grown by chemical bath deposition. *Thin Solid Films* 500:4–8
23. Shayesteh SF, Kolahi S, Kalandarragh YA (2013) Effect of pH on the structural and optical properties of ZnS nanoparticles embedded in PVA matrix. *Ind J Pur Appl Phys* 51:780–783
24. Choudapur VH, Bernal AS, Raju AB (2018) Influence of pH on optoelectronic properties of zinc sulphide thin films prepared using hydrothermal and spin coating method. *Mater Res Expr* 5:045201
25. Akhtar MS, Riaz S, Naseem S (2015) Optical properties of sol-gel deposited ZnS thin films: spectroscopic ellipsometry. *Mater Today Pro* 2:5497–5503
26. Reyes O, Maldonado D, Escorcia-Garcia J, Sebastian PJ (2018) Effect of temperature and pH on direct chemical bath deposition of cuprous oxide thin films. *J Mater Sci Mater Electr* 29:15535–15545
27. El Hamidi A, Meziane K, El Hichou A, Jannane T, Liba A, El Haskouri J, Amorós P, Almaggoussi A (2018) Refractive index controlled by film morphology and free carrier density in undoped ZnO through sol-pH variation. *Optik* 158:1139–1146
28. Hamad S, Cristol S, Richard C, Catlow A (2002) Surface structures and crystal morphology of ZnS: computational study. *J Phys Chem B* 106:11002–11008
29. Aslan F, Tumbul A, Gökteş A, Budakoğlu R, Mutlu İH (2016) Growth of ZnO nanorod arrays by one-step sol-gel process. *J Sol-Gel Sci Technol* 80:389–395
30. Hafeez M, Manzoor U, Bhatti AS, Burak Kaynar M, Ismat Shah S (2011) Catalyst solubility and self-doping in ZnS nanostructures. *J Appl Phys* 110:014317
31. Goktas A, Aslan F, Yasar E, Mutlu İH (2012) Preparation and characterisation of thickness dependent nano-structured ZnS thin films by sol-gel technique. *J Mater Sci Mater Electron* 23:1361–1366
32. Schmidt RL, Kunc K, Cardona M, Bilz H (1979) Second-order Raman scattering in II-VI semiconductors: relative intensities and trends. *Phys Rev B* 20:3345–3350
33. Bouznit Y, Beggah Y, Boukerika A, Lahreche A, Ynineb F (2013) New co-spray way to synthesize high quality ZnS films. *Appl Surf Sci* 284:936–941
34. Lee HJ, Lee SI (2007) Deposition and optical properties of nanocrystalline ZnS thin films by a chemical method. *Curr Appl Phys* 7:193–197
35. Fathy N, Ichimura M (2005) Photoelectrical properties of ZnS thin films deposited from aqueous solution using pulse electrochemical deposition. *Sol Energy Mater Sol Cells* 87:747–756
36. Murase N, Jagannathan R, Kanematsu Y, Watanabe M, Kurita A, Hirata H, Yazawa T, Kushida T (1999) Fluorescence and EPR characteristics of Mn²⁺-doped ZnS nanocrystals prepared by aqueous colloidal method. *J Phys Chem B* 103:754–760